J. Pharm. Pharmacol. 1990, 42: 219–225
Received April 12, 1990

Effects of Compaction Variables on Porosity and Material Tensile Strength of Convex-faced Aspirin Tablets

K. G. PITT†, J. M. NEWTON AND P. STANLEY*

*The School of Pharmacy, University of London, Brunswick Square, London WC1N 1AX and, * Department of Mechanical Engineering, University of Manchester, Manchester M13 9PL, UK*

Abstract—The porosity and tensile strength of convex-faced aspirin tablets formed under a compaction pressure in the range 40–320 MPa and at punch velocities in the range 0·008 to 500 mm s^{-1} have been determined. The material tensile strength, σ_f, was calculated from the observed fracture load, P_s, using the equation of Pitt et al (1988):

$$\sigma_f = \frac{10\,P_s}{\pi D^2}\left(2{\cdot}84\frac{t}{D} - 0{\cdot}126\frac{t}{W} + 3{\cdot}15\frac{W}{D} + 0{\cdot}01\right)^{-1}$$

where D is the tablet diameter, t is the overall tablet thickness and W is the central cylinder thickness. Tablets formed at lower compaction pressures had a higher porosity and lower tensile strength than those formed at higher compaction pressures. Tablets of face curvature ratio (D/R) in the range 0·25–0·67 and a normalized cylinder length (W/D) of 0·2 had the optimum tensile strength. (R is the radius of curvature of the tablet face.) Tablets formed at high compaction rates were significantly weaker than those formed at lower compaction rates.

The effects of altering the compaction rate on the properties of pharmaceutical tablets have been widely investigated. A decrease in the breaking strength of sucrose compacts with an increase in compaction rate was established by Seitz & Flessland (1965). Similar trends have been shown for phenacetin, lactose and microcrystalline cellulose by Hiestand et al (1977) who explained the decrease in terms of a decrease in plastic deformation due to a reduction in the time available for stress relaxation, and for microcrystalline cellulose and phenazone by Ritter & Sucker (1980) who accounted for this trend in terms of a change to a "fragmentation"-type mechanism of bonding.

David & Augsberger (1977) examined various direct compression materials at compression cycle durations of 0·09 and 10 s on a rotary tablet machine. They found no increase in tensile strength for relatively brittle materials, e.g. lactose, but did find an increase in strength for plastically deforming materials, e.g. starch.

Rees & Rue (1978) examined the changes in density caused by altering the contact time, which Jones (1977) described as the total time over which a detectable force is applied to the die contents during compression and decompression. Tablet density increased with an increase in contact time for plastic materials, e.g. microcrystalline cellulose, due to the prolongation of the time for plastic deformation. Brittle materials, e.g. lactose, showed no changes in density with increasing contact time.

Roberts & Rowe (1985) examined the strain sensitivity of pharmaceutical materials over a range of punch velocities from 0·033 to 4000 mm s^{-1} by means of Heckel plots (Heckel 1961a, b). For materials thought to deform plastically, e.g. maize starch, there was an increase in the yield pressure with punch velocity, attributed to a change from ductile to brittle behaviour or to a reduction in the amount of plastic flow. For materials thought to consolidate by fragmentation, e.g. calcium carbonate, there was no change in yield pressure with increasing velocity.

We (Pitt et al 1989b) reported the changes in material tensile strength of convex-faced aspirin tablets compacted at a slow compaction rate of 5 mm min^{-1}. The object of the work described here was to investigate the changes in porosity and material tensile strength of aspirin tablets of different face-curvature and cylinder length compacted at compaction rates similar to those achieved on commercial compression machines.

Materials and Methods

Materials

Crystals from one batch of aspirin (acetylsalicylic acid) (Monsanto, batch number 4B 611, grade 7016) were sieved under identical conditions and the fraction 250–355 μm retained for use. The crystals were stored in amber glass jars with air-tight seals at a temperature of approximately 20°C.

Compaction

Compaction studies in the past have been conducted on reciprocating and on high-speed rotary compression machines. However, instrumenting these machines presents difficulties and only provides information on that particular type of compressor. An alternative approach is to simulate the action of one station of a high-speed compressor using a single punch compressor. Rees et al (1972) devized a

† Present address: Pharmacy Research and Development, Roche Products Ltd, PO Box 8, Welwyn Garden City, Herts AL7 3AY, UK.

Correspondence: J. M. Newton, The School of Pharmacy, 29–39 Brunswick Square, London WC1N 1AX, UK.

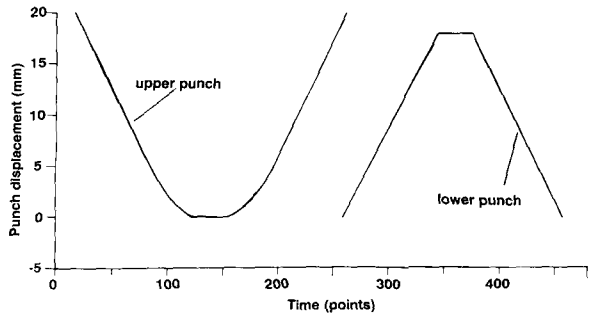

FIG. 1. Compaction and ejection profile.

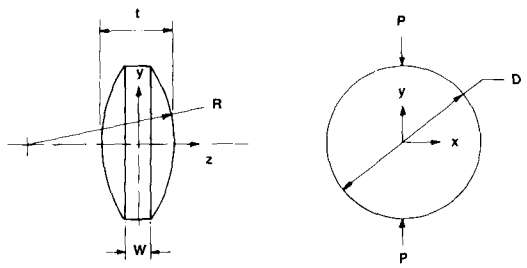

FIG. 2. Side and front elevation of convex-faced disc showing axes and symbols.

technique to simulate the two-sided compaction of a tablet-compressing machine, but it could not reproduce unusual and multiple compression-ejection cycles or operate at high compaction rates.

Hunter et al (1976) showed that hydraulic servo-control could achieve a two-sided compaction using complex punch displacement/time waveforms. A range of cycles could be produced with very high punch velocity and high frequency response.

In the investigation described here, tablets were manufactured using a high-speed compaction simulator based upon a Mand testing machine. The simulator was computer-controlled and could be programmed to follow a defined punch-tip displacement profile. The profile could be arbitrarily defined, e.g. by a sine curve, or could correspond to an actual compression cycle.

Geometric shapes were used to produce a profile D (Fig. 1) which follows a "saw-tooth" profile of simple linear punch movement. Once a profile is defined, the rate of punch movement is dictated by the rate at which the profile is scanned and input into the simulator. The profile D was used in the comparison of the effect of compaction rate on the material tensile strength of tablets of different face-curvatures and cylinder lengths. Seven different face-curvatures were examined (Table 1) and three different cylinder length ratios (W/D) of 0·1, 0·2 and 0·3 (Fig. 2), where W is the central cylinder thickness and D is the tablet diameter.

The optimum punch velocity for tablet formation at a fast compaction rate was determined by scanning the profile over periods of 100, 200 and 2000 ms, giving nominal maximum punch-tip velocities of 1000, 500 and 50 mm s^{-1} as measured from the linear portion of the profile. Convex-faced tablets ("deep curvature", with D/R = 1·25, where R is the radius of curvature of the tablet face, and W/D = 0·2), compacted at 1000 mm s^{-1}, were successfully ejected intact after formation but then "capped" (i.e. the convex-face separated from the cylinder body) on standing, when examined after 2 h, thereby invalidating the determination of tensile strength. This capping would appear to confirm the explanation of Hiestand et al (1977) that weak tablet structures are formed at high compaction rates because of stress relaxation and the breaking of bonds, rather than because of the non-formation of the bonds initially.

Table 1. Face-curvature of tablets.

Face curvature D/R	Curvature description
0	* Flat
0·25	Micro
0·50	* Shallow
0·67	Normal
1·00	* Unity
1·25	* Deep
1·43	* Coating

* corresponds to previous test specimens (Pitt et al 1989a).
D = diameter of tablet (12·5 mm).
R = radius of face-curvature.

Tablets could be formed at 500 mm s^{-1} but had a tendency to cap on diametral testing, particularly the deeper convex-faced tablets, thus invalidating the diametral compression test. The tablets formed at 50 mm s^{-1} were ejected, stored and failed in tension without capping when loaded diametrically; hence this speed, 50 mm s^{-1}, was selected for the characterization of high speed compaction.

Although the selected high speed compaction rate is less than the maximum speed possible on the compaction simulator, this speed does enable tablets to be produced which fail in a reproducible tensile manner, hence allowing comparisons to be made of the material tensile strength of tablets formed at low and high compaction rates. The speed of 50 mm s^{-1} is equivalent to that of a single-punch reciprocating press.

Tablet preparation

The compaction simulator can only follow a punch displacement/time profile; it cannot follow a pressure/time profile. Hence, the simulator pressure could only be adjusted by altering the punch displacement, i.e. the minimum distance between the punch tips during compaction. Pressure and dimension control was therefore effected by a combination of altering the die-fill (Table 2) and the distance between the punch-tips.

The procedure adopted for tablet preparation was to compact 50 tablets for each face-curvature and cylinder length, divided into five batches, compressed at different pressures; these were stored for two weeks and then fractured diametrically (Fell & Newton 1970). The weight (±0·001 g) and overall tablet thickness (±0·001 mm) of each tablet were determined. Pitt (1986) established that only the central cylindrical portion of the tablet changed in dimension when either the weight or the formation pressure changed. Hence measurement of the overall thickness of the tablet reflected changes in the value of W. The value of the height of the curved portion of the tablet ((t − W)/2, where t is the overall

Table 2. Tablet masses, (g, mean of 10 values) at compaction rate of 50 mm s^{-1}. The data for compaction pressures from 55 to 270 MPa are similar to those at 37·5 MPa.

Lower compaction pressure (MPa)	Face curvature ratio D/R	Cylinder length ratio W/D 0·1	0·2	0·3
37·5	0	0·189	0·394	0·587
	0·25	0·250	0·441	0·643
	0·50	0·312	0·507	0·706
	0·67	0·346	0·574	0·751
	1·00	0·441	0·644	0·847
	1·25	0·494	0·709	0·909
	1·43	0·616	0·819	*
300	0	#	0·404	0·610
	0·25	0·255	#	0·661
	0·50	0·312	0·518	0·719
	0·67	0·361	0·569	#
	1·00	#	0·655	0·870
	1·25	0·507	0·725	#
	1·43	#	#	*

* no data available (tablets too thick for storage cassette).
# no tablets formed at this pressure.
D = diameter of tablet (12·5 mm).
R = radius of face curvature.
W = cylinder length.

tablet thickness), was measured for each face curvature, from a magnified image of the tablets.

The die was filled by means of a hopper, under automatic control, which shuffled back and forth over the die at the beginning of the compaction cycle. The pressure derived from the force recorded on the lower punch was used as a characteristic of the formation process. Although the coefficient of variation of the die fill weight was low (ca 0·5%), this was sufficient to cause scatter of the formation pressures within a batch (Fig. 3). This scatter made interpretation of the data difficult as there was no clearly defined fracture load for a given pressure and a specified W/D. Some processing of

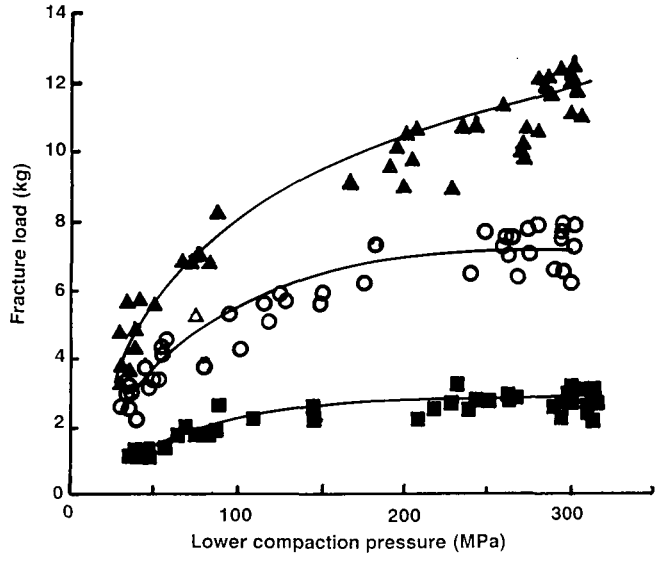

FIG. 3. Fracture load versus lower compaction pressure. Compaction rate = 50 mm s^{-1}. D/R = 0·5, □ W/D = 0·1, + W/D = 0·2, △ W/D = 0·3.

Table 3. Summary of degree of polynomial fit for fast compaction data. (Fracture load with compaction pressure.)

Face-curvature D/R	Cylinder length ratio (W/D) 0·1	0·2	0·3
0	1	1	3
0·25	2	2	5
0·50	2	2	2
0·67	2	2	5
1·00	2	2	5
1·25	2	2	5
1·43	4	4	*

* no data available (tablets too thick for collection cassette).
D = diameter of cylinder (12·5 mm).
R = radius of face-curvature.
W = cylinder length.

the data points was therefore necessary. One approach was to fit a polynomial to the data values. However, the degree of the polynomial would affect the calculation of the fitted values, and so a logical and consistent method had to be developed to assist in the selection of the polynomial of optimum degree. This was accomplished by means of orthogonal polynomials (Snedecor & Cochrane 1980) using the method of Forsythe (1957) in the form of the computer program BMDP5R (Biomedical Computer Programs, University of California).

This analysis can be considered as a method of comparing the residuals of the fitting process by means of a *t*-test. The residual values from the fitting of successive polynomials of increasing degree are compared and the point at which the difference in residuals between two successive polynomial fittings is no longer significant is assessed. The polynomial for which this difference in residuals is no longer significant is deemed to be the polynomial giving the optimum fit.

The coefficients of the polynomial of the required degree are then calculated and used to fit a curve through the data. The equation of the polynomial is then used to calculate values for the fracture loads at set pressures to allow the comparison of the different specimens.

The results in Table 3 illustrate the degree of the polynomial selected in each case. Most of the results were defined by a quadratic function.

Porosity calculation

The porosity (ε) of each tablet was derived from the dimensions (and hence the volume, V) and mass (M) of the tablet, and the density of the aspirin crystals (ρ), using the expression:

$$\varepsilon = 1 - (M/V)/\rho \qquad (1)$$

Tensile strength calculation

After ejection, the tablets were stored in air-tight amber glass jars for 14 days. The tablets were then weighed and the dimensions recorded before loading diametrically in a CT40 tablet tester (Engineering Systems, Nottingham, UK). Steel platens were used and the crosshead movement rate was 1 mm min^{-1}. Any tablet which did not fail diametrically in tension was excluded from all future calculations.

The fracture loads of the tablets must be converted to material tensile strength values to allow a valid comparison between different-shaped tablets (Pitt et al 1989b).

The material tensile strength (σ_f) of the plane-faced tablets was calculated from equation 2 (Fell & Newton 1970).

$$\sigma_f = \frac{2P}{\pi Dt} \quad (2)$$

This equation can be derived theoretically (Den Hartog 1952); the validity has been confirmed by photoelastic analysis (Frocht 1948). A theoretical solution for discs with convex faces is not available, but Pitt et al (1989a) have established an empirical solution which has been confirmed by using homogeneous brittle test specimens formed from gypsum (Pitt et al 1988). The equation expresses the material tensile strength of the specimen, σ_f, in terms of the fracture load, P_s, disc diameter, D, overall thickness, t, and cylinder length, W, in the form:

$$\sigma_f = \frac{10 P_s}{\pi D^2}\left(2{\cdot}84\frac{t}{D} - 0{\cdot}126\frac{t}{W} + 3{\cdot}15\frac{W}{D} + 0{\cdot}01\right)^{-1} \quad (3)$$

This equation has been found to be valid for convex-faced tablets with values of W/D in the range 0·1 to 0·3 and D/R ratios of 0 to 1·43 (Fig. 2). Values of fracture load, at set intervals of lower compaction pressure, were calculated from the relevant polynomial describing the compaction pressure/fracture load relationship and were converted to material tensile strength values using the above equation.

Results and Discussion

The results in Table 4 are for plane-faced tablets and give values of compaction pressure, porosity and material tensile strength. These results illustrate that for any given pressure there can be different tensile strengths and ejected tablet porosities according to the thickness of the tablet.

Table 4. Summary of compaction data for plane-faced tablets prepared at a compaction rate of 50 mm s^{-1}.

Cylinder length ratio (W/D)	Lower compaction pressure (MPa)	Porosity	Material tensile strength (MPa)
0·1	37·5	0·121	0·102
0·2	37·5	0·083	0·542
0·3	37·5	0·089	0·519
0·1	55·0	0·118	0·153
0·2	55·0	0·082	0·588
0·3	55·0	0·085	0·613
0·1	75·0	0·117	0·212
0·2	75·0	0·082	0·640
0·3	75·0	0·080	0·711
0·1	112·5	0·114	0·322
0·2	112·5	0·075	0·738
0·3	112·5	0·068	0·724
0·1	150·0	0·105	0·432
0·2	150·0	0·069	0·837
0·3	150·0	0·056	1·005
0·1	225·0	0·100	0·651
0·2	225·0	0·065	1·033
0·3	225·0	0·056	1·259
0·1	270·0	0·092	0·782
0·2	270·0	0·063	1·151
0·3	270·0	0·054	2·286
0·1	300·0	*	*
0·2	300·0	0·060	1·230
0·3	300·0	0·053	2·864

* tablets fractures on ejection.
D = diameter of cylinder (12·5 mm).
W = cylinder length.
Values of material tensile strength are calculated from fitted values of fracture load.

The relationship between porosity, ε, and material tensile strength, σ_f, (equation 4) prepared by Ryshkewitch (1953) was shown by linear regression analysis to give the best correlation for the data and hence was used to assess the data.

$$\varepsilon \propto \ln \sigma_f \quad (4)$$

Triple axis plots of porosity, ln (material tensile strength) and compaction pressure are presented in Fig. 4. These show that at low compaction pressure there is high porosity and low material tensile strength and at high compaction pressure there is low porosity and high material tensile strength. Porosities decrease with increasing compaction pressure; as porosity increases the material tensile strength increases. The results for W/D = 0·1 are seen to be anomalous when compared with those of the W/D = 0·2 and W/D = 0·3 tablets in that the porosities of the W/D = 0·1 tablets for a given compaction pressure are much lower than those of the other tablets. At high compaction pressure and low porosities the relationship between porosity and ln (material tensile strength) ceases to be linear, indicating a change in structure and fracture mode at higher compaction pressures. Hence, analysis of the data was confined to the linear, lower pressure range of the graphs. Analysis of the linear portion of these plots was undertaken by linear regression analysis, the parameters of which are shown in Table 5.

Examination of the parameters of the linear regression analysis for porosity and ln (material tensile strength) shows differences in strength for the different dimensions.

The W/D = 0·1 tablets show relatively poor correlation between porosity and ln (material tensile strength), particularly for the low and the smaller D/R values where the value of the correlation coefficient is low and the probability that the relationship is not linear is comparatively high. This could be due to several factors. For example, the compaction process, with variations in the die fill and powder movement, could be involved. There would be a more pronounced powder movement in the deep concave punch faces than the shallower concave ones. Similarly, there are likely to be differences between the two caps as the mechanism of powder filling is different. The lower cap is filled directly by powder settling and the upper one has to be filled by powder movement upwards during the compression cycle. The extent of these differences will vary between the different curvatures. The W/D = 0·1 plane-faced tablets appear to have a higher inherent strength (as indicated by the intercept value, the material tensile strength at zero porosity) than the W/D = 0·2 and W/D = 0·3 plane-faced tablets. It is noteworthy that the W/D = 0·1 tablets did not fail in the same manner as the others; severe deformation preceded failure. This deformation would be expected to reduce the material tensile stresses in the tablets thereby increasing the apparent material tensile strength. A different problem may be present in the W/D = 0·1, D/R = 1·43 tablets; although only tablets which failed in tension were included in the analysis, there was extensive capping with the other tablets in the batch, indicating the possibility of flaws and weaknesses within the tested tablets. This was not seen with the shallower faced tablets. Hence, the tablets which did fail in tension may have

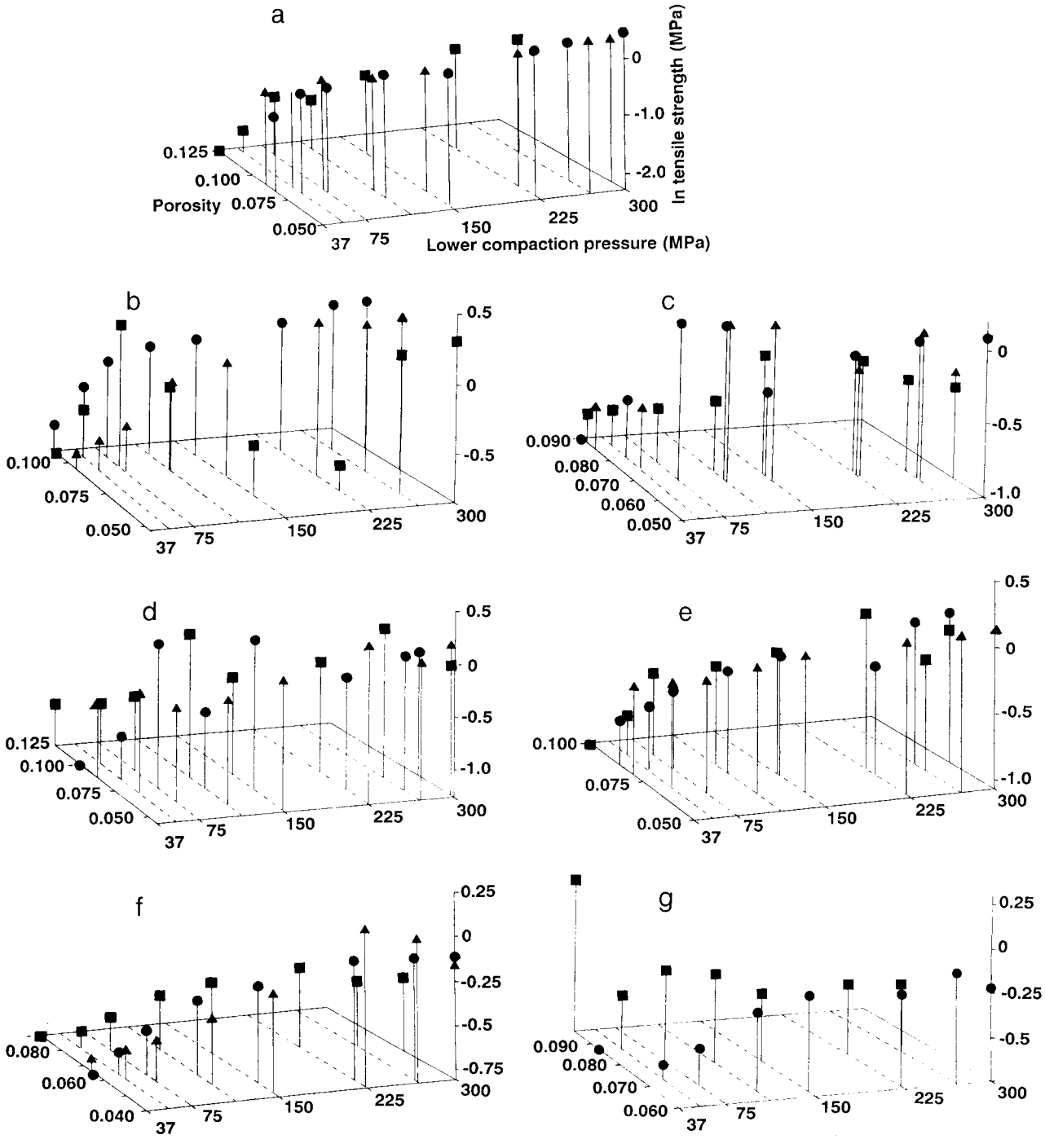

FIG. 4. Triple axis plot of lower compaction pressure, ln (tensile strength) and porosity. Compaction rate = 50 mm s^{-1}, D/R = 0, ■ W/D = 0·1, ● W/D = 0·2, ▲ W/D = 0·3. The labels for all triple axis plots are as shown for a. Separate plots correspond to the following D/R ratios: a, 0; b, 0·25; c, 0·5; d, 0·67; e, 1·0; f, 1·25; g, 1·43.

been weakened during compaction. Therefore there appears to be no correlation between porosity and ln (material tensile strength) for these tablets, due to the presence of irregular failure planes within the tablets.

The intercept values in Table 5 indicate that the face-curvature ratios for optimum material tensile strength are D/R = 0·25 to 0·67, (i.e. micro to normal), and that the optimum cylinder length ratio is 0·2. This is illustrated graphically in Fig. 5, which is a plot of ln (material tensile strength) versus compaction pressure, and by the triple axis plot in Fig. 6, which shows, for W/D = 0·2, that tablets with D/R = 0·2 have the greater strength compared with plane-faced (D/R = 0) tablets or tablets with D/R = 1·43 for a given porosity and pressure. Fig. 4a illustrates that plane-faced tablets with W/D = 0·2 have a somewhat greater strength than those with W/D = 0·1 and W/D = 0·3, thus indicating a

Table 5. Summary of linear regression analysis of porosity and ln (material tensile strength) for differing face-curvatures. Compaction rate = 50 mm s^{-1}.

Face-curvature ratio (D/R)	Cylinder length ratio (W/D)	Correlation coefficient	Probability	Gradient	Intercept ln(MPa)
	0·1	−0·9748	$0·19 \times 10^{-3}$	−70·2	6·42
0	0·2	−0·9854	$0·77 \times 10^{-3}$	−38·3	2·53
	0·3	−0·9622	$0·13 \times 10^{-3}$	−25·9	1·68
	0·1	−0·5619	0·15	−19·4	1·05
0·25	0·2	−0·9710	$0·59 \times 10^{-4}$	−49·4	4·79
	0·3	−0·9849	$0·85 \times 10^{-5}$	−46·9	3·71
	0·1	−0·4461	0·27	−11·2	0·42
0·50	0·2	−0·8583	$0·64 \times 10^{-2}$	−33·7	2·05
	0·3	−0·8108	$0·14 \times 10^{-1}$	−35·7	2·18
	0·1	−0·8817	$0·38 \times 10^{-2}$	−18·1	1·19
0·67	0·2	−0·8520	$0·72 \times 10^{-2}$	−27·2	1·55
	0·3	−0·8888	$0·75 \times 10^{-2}$	−15·6	0·71
	0·1	−0·8953	$0·65 \times 10^{-2}$	−23·7	1·42
1·0	0·2	−0·9776	$0·28 \times 10^{-4}$	−49·7	3·46
	0·3	−0·9810	$0·16 \times 10^{-4}$	−20·9	1·19
	0·1	−0·9291	$0·85 \times 10^{-3}$	−16·1	0·57
1·25	0·2	−0·9610	$0·14 \times 10^{-3}$	−27·8	0·99
	0·3	−0·9930	$0·72 \times 10^{-4}$	−24·4	0·74
1·43	0·1	−0·7436	$0·55 \times 10^{-1}$	−18·3	−1·74
	0·2	−0·9099	$0·17 \times 10^{-2}$	−23·3	1·14

D = diameter of cylinder (12·5 mm).
R = radius of face-curvature.
W = cylinder length.
Probability is the probability that this relationship occurred by chance.
Values of material tensile strength are calculated from fitted values of fracture load.

complex relationship between the movement of powder during compaction, specimen dimensions and material tensile strength.

The change in compaction mechanism with increasing cylinder length and differing face-curvature is illustrated by the changes in the degree of polynomial required to give the optimum fit to the fracture load/compaction pressure plots

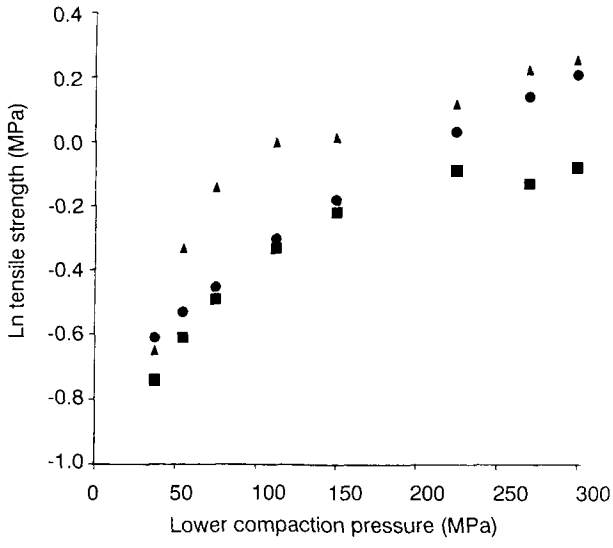

FIG. 5. Ln (tensile strength) versus lower compaction pressure. Compaction rate = 50 mm s^{-1}, D/R = 0·2, ● = 0 W/D, ▲ = 0·25 W/D, ■ = 1·25 W/D.

Table 6. Material tensile strength of plane-faced aspirin tablets (n = 10) at different punch velocities at a compaction pressure of 150 MPa.

Punch velocity (mm s^{-1})	Material tensile strength (MPa)	CV (%)
0·0083	1·80	8·1
0·083	1·88	8·0
0·33	1·76	7·9
0·83	1·78	5·1
50·0	1·00	10·0
500·0	0·60	15·0

CV = coefficient of variation of material tensile strength.

(Table 3). This table shows that the data for the plane-faced tablets with W/D = 0·1 and 0·2 were best described by means of a linear relationship, whereas the data for the corresponding convex-faced tablets were generally best fitted by a quadratic function. The quadratic function was required to describe the decreased fracture load at high pressures, associated with the tendency towards "capping" of the convex-faced tablets. Tablets with W/D = 0·3 or D/R = 1·43 required a far more complex equation, up to degree 5, to describe the fracture load/pressure profile, indicating that more factors were affecting the strength of these tablets.

One factor could be the increased stress relaxation that occurred after formation of tablets at high pressure. There was no measurable dimensional change over the 2 week period for the tablets compacted at lower pressures, where equation 4 was applicable, whereas those tablets compacted at high pressures expanded during storage. Photographic examination indicated that this expansion, up to 5% axially, occurred only in the cylindrical portion of the tablet. Hence this expansion of the tablet would appear to have weakened the bonds within the tablets, resulting in flaws in the compact. This again would agree with the observation of Hiestand et al (1977) that weakness of tablets compacted at high speeds can be attributed to the breaking of bonds rather than the lack of time to form them.

The effect of compaction rate

The tablets formed at high compaction rates were significantly weaker than those formed at slow compaction rates (Table 6). It is of interest that for the first 100-fold increase in punch-tip velocity (from 0·0083 to 0·83 mm s^{-1}) there was no significant change in material tensile strength, whereas for the next increase in punch-tip velocity (a 60-fold increase to a velocity equivalent to that of a single punch tableting machine), there was a significant difference in material tensile

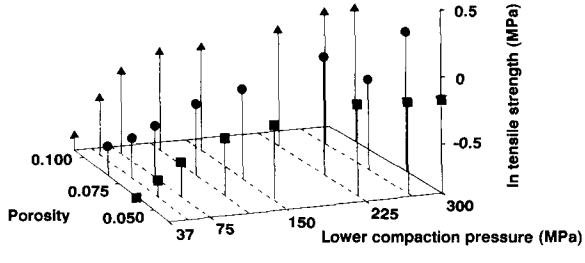

FIG. 6. Triple axis plot of lower compaction pressure, ln (tensile strength) and porosity. Compaction rate = 50 mm s^{-1}, W/D = 0·2, ● = 0 D/R, ▲ = 0·25 D/R, ■ = 0·3 D/R.

strength. This was also the case for the next increase in punch-tip velocity (a 10-fold increase in velocity to the equivalent of that of a rotary machine). Thus, tableting-rate-related changes in the strength of aspirin only become significant in the region over which tableting machines operate.

Conclusions

This high speed compaction study has shown that there are complex relationships between material tensile strength, compaction pressure and porosity. The results indicate the heterogeneous nature of tablets produced by compaction. The tensile strength of a convex-faced tablet formed at fast compaction rates can be assessed by equation 3. However, these tablets have different porosities and so are not being compared under the same material conditions. Hence, to determine the effect of face-curvature upon the mechanical strength of the compacts, the tablets were compared in a manner which is free from specimen-dependent effects. This was best achieved by linear regression analysis of porosity and natural log (material tensile strength).

This approach has shown that there are optimum face-curvatures and cylinder lengths for the greatest mechanical strength. The differences in compaction mechanisms between one face-curvature and another are indicated by the changing value for the degree of the polynomial required to fit the fracture load/lower compaction pressure profile. Some of the factors causing these differences have been suggested previously. The position in the die at which the tablet is formed will affect the material tensile strength of the ejected tablet due to possible air entrapment or ejection damage. Stress relaxation must play a part in the determination of the structure and hence material tensile strength of the tablet, as indicated by the spontaneous capping of the tablets manufactured at 1000 mm s^{-1} following 2 h storage. The capping of the tablets also indicated the differences in structure between the upper and lower caps as it was always the upper cap which parted from the cylinder body. Thus, equations 2 and 3 can be used to assess the material tensile strength of convex-shaped tablets compacted at high speed, but any comparison of material tensile strength must allow for the compaction conditions under which the tablets were formed.

Acknowledgements

The authors would like to thank Boots Company plc (in particular Dr R. Richardson) for the provision of materials and access to the compaction simulator, and SERC for providing a research studentship for K.G.P.

References

David, S. T., Augsberger, L. L. (1977) Plastic flow during compression of directly compressible fillers and its effect on tablet strength. J. Pharm. Sci. 66: 155–159

Den Hartog, J. P. (1952) Advanced Strength of Materials. McGraw Hill, New York

Fell, J. T., Newton, J. M. (1970) Determination of the mechanical strength of tablets by the diametral compression test. J. Pharm. Sci. 59: 688–691

Forsythe, G. E. (1957) Generation and use of orthogonal polynomials for data fitting with a digital computer. J. Soc. Ind. Appl. Math. 5: 74–88

Frocht, M. M. (1948) Photoelasticity. Vol II. John Wiley and Sons Inc., New York

Heckel, R. W. (1961a) Density-pressure relationships in powder compaction. Trans. Met. Soc. RIME 221: 671–675

Heckel, R. W. (1961b) An analysis of powder compaction phenomena. Ibid. 221: 1001–1008

Hiestand, E. N., Wells, J. E., Poet, C. B., Ochs, J. F. (1977) Physical processes of tabletting. J. Pharm. Sci. 66: 510–519

Hunter, B. M., Fisher, D. G., Pratt, R. M., Rowe, R. C. (1976) A high-speed compaction simulator. J. Pharm. Pharmacol. 28 (Suppl): 65P

Jones, T. M. (1977) Formulation factors: drugs given by oral route. In: Polerman, J. (ed.) Formulation and Preparation of Dosage Forms. Elsevier, North Holland, pp 29–44

Pitt, K. G. (1986) Mechanical Strength of Convex-faced Round Tablets. Ph.D. thesis, University of London

Pitt, K. G., Newton, J. M., Stanley, P. (1988) Tensile fracture of doubly-curved cylindrical discs under diametral loading. J. Mat. Sci. 28: 2723–2728

Pitt, K. G., Newton, J. M., Stanley, P. (1989a) Stress distributions in doubly-convex cylindrical discs under diametral loading. J. Phys. (D) 22: 1114–1127

Pitt, K. G., Newton, J. M., Richardson, R., Stanley, P. (1989b) The material strength of convex-faced aspirin tablets. J. Pharm. Pharmacol. 41: 289–292

Rees, J. E., Rue, P. J. (1978) Time-dependent deformation of some direct compression excipients. Ibid. 30: 601–607

Rees, J. E., Hersey, J. A., Cole, E. T. (1972) Simulation device for preliminary tablet compression studies. J. Pharm. Sci. 61: 1313–1315

Ritter, A., Sucker, H. B. (1980) Studies of variables that affect tablet capping. Pharm. Tech. 4: 56–65

Roberts, R. J., Rowe, R. C. (1985) The effect of punch velocity on the compaction of a variety of materials. J. Pharm. Pharmacol. 37: 377–384

Ryshkewitch, E. (1953) Compression strength of porous sintered alumina and zirconia. J. Am. Chem. Soc. 36: 65–68

Seitz, J. A., Flessland, G. M. (1965) Evaluation of the physical properties of compressed tablets I: tablet hardness and friability. J. Pharm. Sci. 55: 1353–1357

Snedecor, G. W., Cochrane, W. G. (1980) Statistical Methods 7th edn, Iowa State University Press